PAPER

Study of the early growth stages of chemically deposited ZnS thin films from a non-toxic solution

Materials Research Express

PAPER

Study of the early growth stages of chemically deposited ZnS thin films from a non-toxic solution

RECEIVED
2 May 2018

REVISED
20 June 2018

ACCEPTED FOR PUBLICATION
29 June 2018

PUBLISHED
11 July 2018

C A Rodríguez[1,2,8], M Flores[3], M Sandoval-Paz[4], M P Delplancke[5], G Cabello–Guzmán[6] and C Carrasco[7,8]

[1] Multidisciplinary Research Institute for Science and Technology, Ineergias, University of La Serena, 980 Benavente St., La Serena, Chile
[2] Department of Chemistry, Faculty of Sciences, University of La Serena, Campus Andrés Bello, 1305 Raúl Bitrán St., La Serena, Chile
[3] Department of Physics, Faculty of Physical and Mathematical Sciences, University of Chile, 850 Beauchef St., Santiago, Chile
[4] Department of Physics, Faculty of Physical and Mathematical Sciences, University of Concepción, Esteban S. Iturra Av., Concepción, Chile
[5] 4MAT, Université Libre de Bruxelles, 50 Roosevelt Av., CP 165/63, Brussels 1050, Belgium
[6] Department of Basic Sciences, Faculty of Sciences, University of Bío-Bío, Campus Fernando May, Chillán, Chile
[7] Department of Materials Engineering, University of Concepción, 270 Edmundo Larenas St., Concepción, Chile
[8] Authors to whom any correspondence should be addressed.

E-mail: arodriguez@userena.cl **and** ccarrascoc@udec.cl

Keywords: ZnS thin films, growth stages, chemical bath deposition, XPS, AFM

Abstract

ZnS thin films grown by the chemical bath deposition method have been under intense investigation due to their applications in solar cells. In this work, the early growth stages of ZnS thin films deposited by means of a non-toxic solution are studied by measuring the morphological, chemical and optical properties of the films obtained at different deposition time (5, 10, 20, 30, 60, 90 and 120 min). From the atomic force microscopy (AFM) studies, it was seen that the substrate surface is not fully covered before 20 min, and the growth exponential value changed from 0.5 to 1.8. The x-ray photoelectron spectroscopy (XPS) measurements revealed the presence of the Zn–O bond and the absence of the S–Zn bond at the earliest deposition time. Additionally, from XPS analysis, a shift in the signals for O1s and Zn2p$_{3/2}$ for the sample grown at 30 min was observed due to the formation of Zn(OH)$_2$. Finally, the UV-Vis spectrophotometry measurements showed that all samples have a high transmittance (>80%) and that the band gap value decreased as the deposition time increased.

1. Introduction

Zinc sulfide (ZnS) thin films have been under intense investigation due to their excellent optical properties [1–3]. Among the different applications of ZnS, it has shown significant potential for use as a buffer layer in thin-film solar cells (TFSCs). The high optical transmission, wide band gap and low toxicity and cost have made this material the best choice to replace CdS, which is the most used buffer layer in TFSCs [4].

There are several methods to deposit ZnS thin films. Among them, chemical bath deposition (CBD) has risen in popularity because it is a simple and inexpensive technique for the deposition of semiconductor materials to be used in TFSC devices. In addition, the best conversion efficiency for Cu(In, Ga)Se$_2$-based solar cells has been reached using a buffer layer grown by CBD [5], due to the less abrupt p-n junction produced by this method compared with other techniques [6]. The reaction solution to deposit ZnS thin films normally include one or more complexing agents, where ammonia (NH_4) and/or hydrazine (N_2H_4) are the most used. It is well known that ammonia and hydrazine are highly volatile materials that are toxic and harmful to the environment and human health.

Alternatively, although ZnS thin films have been widely deposited by CBD, there are only a few works related to the growth mechanism and its influence on the film properties [2, 7]. The growth of a film by means of CBD is characterized by an induction time and two distinct growth mechanisms; the first one is the ion-by-ion mechanism and the second one correspond to the cluster-by-cluster mechanism. In the ion-by-ion growth mechanism, the film formation proceed by a direct ion reaction (for example, Zn^{2+} reacts with S^{2-} to form

ZnS); however, in the cluster-by-cluster mechanism, the films formation proceed through an intermediate specie (for example, $Zn(OH)_2$ reacts with S^{2-} to form ZnS). The predominance of one mechanism over the other is a topic of continuous discussion. The influence of temperature [2], solution pH [8], source of Zn^{2+} ions [9] and bath composition [10] on the growth mechanism during the deposition of ZnS thin films has been studied. However, the evolution of the growth film mechanism as a function of time for the non-toxic deposition of ZnS thin films has been not reported yet. The initial growth stages of the reaction solution determine the evolution of different stages during the CBD process [11], affecting the morphological, chemical and optical properties of the film. On this basis, an analysis of film formation as time proceeds would be useful to optimize the properties of the film.

In our previous study, we reported the synthesis and characterization of ZnS thin films through a non-toxic chemical bath, where ammonia and hydrazine were replaced by sodium citrate and tartaric acid as non-toxic complexing agents. In addition, potassium hydroxide was used as a pH adjuster [4]. The growth process was performed by multiple depositions on a single substrate (grown several times), in order to obtain thicker films. From chemical analysis, the presence of ZnO was only found in the first deposited layer (where the ZnS thin films were grown directly on the glass substrate), and the presence of a high amount of $Zn(OH)_2$ was detected in all samples, as a consequence of the predominance of the cluster-by-cluster mechanism. The presence of ZnO during the deposition of ZnS thin films has been reported previously [12]. Nevertheless, the appearance of ZnO only in the first layer is an intriguing phenomenon to address, due to the interesting potential of the ZnS/ZnO system in photovoltaic applications. In the present work, we studied the morphological, chemical and optical properties at the early growth stages of chemically deposited ZnS thin films, in order to elucidate two interesting features: (i) the presence of ZnO in the thinner film and (ii) the growth mechanisms with increasing deposition time, which can be used to optimize the deposition time of ZnS films for applications as buffer layers in TFSCs.

2. Experimental

The procedure to deposit ZnS thin films from a non-toxic alkaline solution is described in [4], which is based on a mixture of heptahydrated zinc sulfate, sodium citrate dehydrate, tartaric acid and thiourea. The volume of solution reaction was 100 mL, completed by adding deionized water. The pH was adjusted to 10.5 by adding KOH (Sigma–Aldrich, 85% purity) and a buffer solution of pH 10. Initially, the substrates were cleaned as reported elsewhere [4]. After that, the substrates were immersed vertically on the reaction solution at 75 °C. The temperature was maintained constant during all the deposition process and the reaction solution was not stirred. Seven samples were grown at the times of 5, 10, 20, 30, 60, 90 and 120 min. After the corresponding deposition time, samples were removed, rinsed with deionized water, dried at room temperature and stored in a dry place.

The surface morphology was studied by means of atomic force microscopy (AFM) using an Omicron SPM1 equipment running in vacuum conditions with a PPP–CONTR tip and radius of curvature 10 nm. The surface roughness (RMS) of thin films was calculated using WSxM software [13] over $2.5 \times 2.5\ \mu m^2$ images (measured at least twice). The chemical composition of the ZnS thin films was measured by means of x-ray photoelectron spectroscopy (XPS), with an XPS–Auger PerkinElmer spectrometer model PHI 1257 using a monochromatic Al x-ray source ($h\upsilon = 1486.6$ eV). Finally, the optical transmittance of the ZnS thin films grown on quartz slides [4] was measured at room temperature using a Jasco UV–VIS spectrophotometer model V–530 with a 1 nm resolution.

3. Results and discussion

3.1. Chemical reactions of ZnS formation

The ZnS film formation through CBD is a controlled precipitation process that involves several chemical reactions. In this work, synthesis of the ZnS thin films was performed through a non-toxic solution using sodium citrate dehydrate and tartaric acid as a mixture of non-toxic complexing agents. The pH was adjusted by adding KOH. Therefore, the Zn^{2+}, OH^- and S^{2-} ions are released to form $ZnS_{(s)}$.

In the presence of the complexing agents sodium citrate (CIT) and tartaric acid (TA), Zn^{2+} ions are complexed and the ZnS formation occurs through the following reactions:

$$Zn(CIT)_n^{2-n} \leftrightarrow Zn_{(aq)}^{2+} + nCIT_{(aq)}^{3-} n = 1, 2 \quad (1)$$

$$Zn(TA)_{(aq)} \leftrightarrow Zn_{(aq)}^{2+} + TA_{(aq)}^{2-} \quad (2)$$

$$Zn_{(aq)}^{2+} + S_{(aq)}^{2-} \rightarrow ZnS_{(s)} \quad (3)$$

In alkaline solution, Zn–OH species are also formed and obtaining ZnS can also proceed through an ionic exchange between $Zn(OH)_2$ and S^{2-} ions as follows:

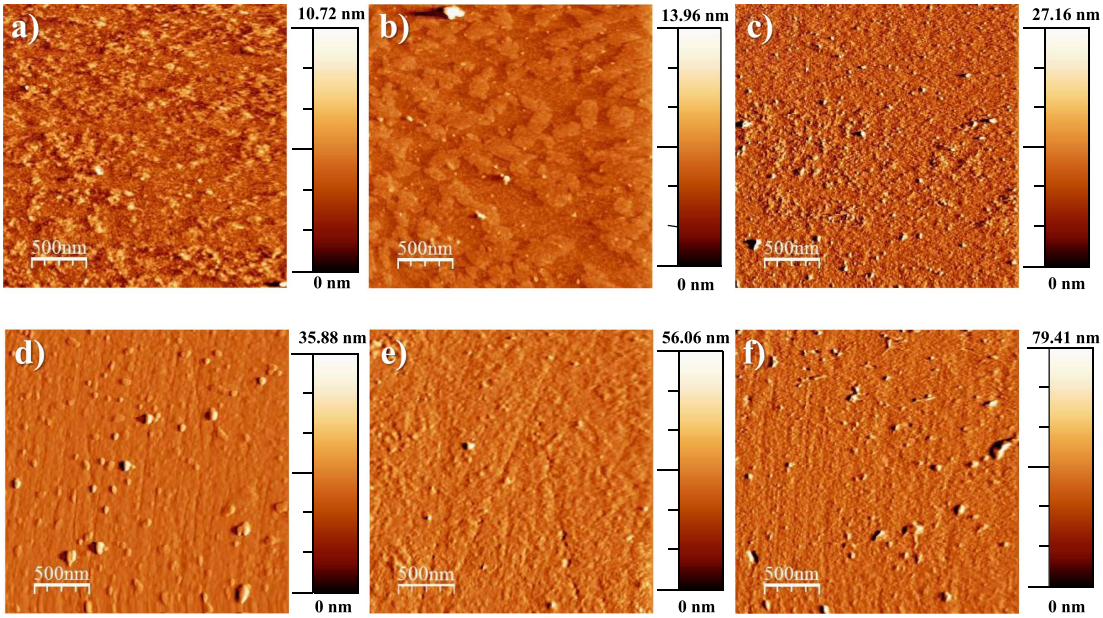

Figure 1. Typical 2.5 × 2.5 μm^2 AFM images of ZnS thin films deposited at (a) 5, (b) 10, (c) 20, (d) 30, (e) 90 and (f) 120 min.

$$Zn(OH)_2 + S^{2-} \rightarrow ZnS_{(s)} + 2OH^- \quad (4)$$

Equations (3) and (4) corresponds to the ion–by–ion and cluster–by–cluster growth mechanisms. In the ion–by–ion mechanism the Zn^{2+} ions are released from the complexes to directly react with S^{2-} ions to form $ZnS_{(s)}$. In the cluster–by–cluster mechanism, $ZnS_{(s)}$ is formed by an ion exchange between OH^- and S^{2-} ions [14].

The stability constants of Zn-citrate complexes ($pK_1 = 4.98$ and $pK_2 = 5.90$ [15]) are higher than the corresponding value for Zn-tartrate ($pK = 2.68$ [16]). This indicates that, in our system, most of the Zn^{2+} ions are complexed by citrate anions. However, it has been demonstrated that the usage of a second complexing agent during the chemical deposition of ZnS thin films and other similar systems improves the homogeneity of the film [17–20].

3.2. Film morphology

The surface characteristics at the initial formation stages of ZnS thin films were analyzed by means of AFM in contact mode over areas of 2.5 × 2.5 μm^2. Figure 1 shows topographic AFM images of ZnS thin films grown at different deposition time. From figures 1(a) and (b), it can be seen that at 5 min there is a large density of isolated particles with very small sizes and irregular shapes, and such nanostructures are increased in size likely due to a coalescence process at 10 min. It is clear that in the first 10 min of deposition time, there is no formation of a homogenous and compact film on the substrate surface. This growth process is similar to that reported previously for the initial growth stages of CdS films [21].

At 20 min of deposition time (figure 1(c)), a compact and homogeneous film is observed which is formed by very small and smooth grains covering the surface substrate. However, a small amount of aggregates are also observed (larger clear particles.). At 30 min and thereafter (figures 1(d)–(f)), the deposited samples exhibited a similar surface characteristic to the samples grown at 20 min, i.e., homogenous and compact films covering the entire substrate surface, where larger aggregates can be seen.

It is also observed for samples grown at deposition time of 30, 90 and 120 min, the presence of lines like scratches which are attributed to the substrate surface characteristics.

In a growth process where the film thickness, h, is proportional to the deposition time, t (within the asymptotical limits), the roughness variation is given by the following power law [22, 23]:

$$RMS(h) = ah^{\beta} \quad (5)$$

where 'a' is a proportionality constant and β is the growth exponent.

In order to follow the film morphology evolution, the growth exponent was obtained by performing a linear fit with the Origin® software from the graph log (RMS) versus log (deposition time), and the values are shown in figure 2. The RMS value of the clean substrate was 0.42 nm (not included in figure 2). The deposition time dependence of the RMS value, which increases from 0.90 to 2.73 nm, is evidenced. The interesting feature of the results exhibited in figure 2 is the inflection point at 30 min that results in a change in the growth exponent. By

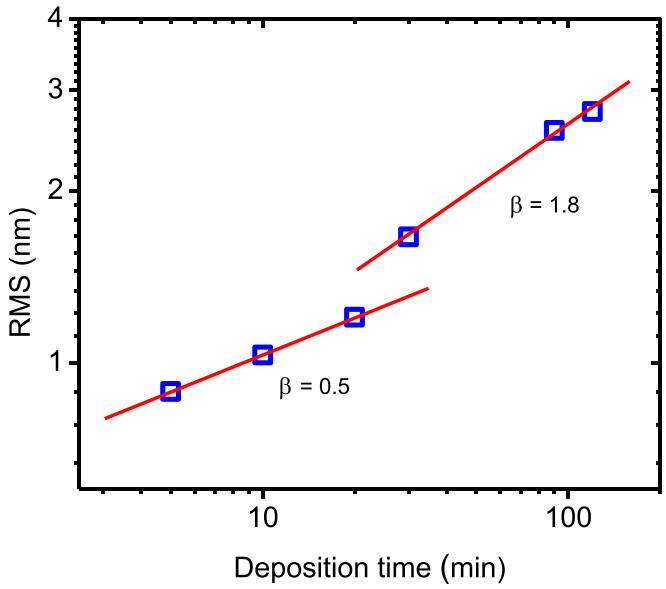

Figure 2. RMS roughness versus deposition time for ZnS thin films grown at different deposition times.

the incorporation of the material in the substrate surface, the slope is $\beta = 0.5$ at the earliest time. For the posterior time, there is a change in the slope, where $\beta = 1.8$. The change of the value of β is a consequence of the modification in the growth mechanism at 30 min (or at some point between 20 and 30 min). Thus, the morphological characteristics of the films give information regarding the growth mechanism. While a surface covered by a homogeneous and continuous film with small and smooth grains has been attributed to the ion-by-ion mechanism, the presence of cluster agglomerations at the surface is attributed to the cluster-by-cluster mechanism [4, 21, 24]. On this basis, the surface features of the obtained films suggest that the deposition process at early growth stages (up to 20 min) is carried out through the ion-by-ion mechanism and then, the film formation proceed mainly through the cluster-by-cluster mechanism. This is in agreement with the values of β, where the larger value of this parameter mainly specifies the rapid roughening of the surfaces, which arises due to the upright growth of aggregates [23].

3.3. XPS analysis

The chemical composition of the thin films and their chemical state were determined through XPS. All the spectra measured were calibrated in energy at the binding energy of C1s, 284.5 eV, attributed to the adventitious carbon. From the full range spectra (not included here), only zinc (Zn), oxygen (O), sulfur (S) and carbon (C) species were identified. Figure 3 shows the high-resolution spectra of the O1s, Zn2p$_{3/2}$ and S2p signals for ZnS thin films grown at different deposition time. For samples grown at 5 and 10 min of deposition time, figures 3(a) and (b), the O1s signal was fitted using four peaks centered at 530.0–530.7 eV, 531.3 $\pm$ 0.1 eV, 532.6 $\pm$ 0.1 eV and 533.4 $\pm$ 0.1 eV binding energies. The first peak can be ascribed to the O–Zn bond [25], the second one corresponds to O–Al bonds [26], the third one is attributed to the O–Si bonds [27] and the last one is normally attributed to the C–O bond and/or adsorbed water [25, 28]. The bonds involving Al and Si correspond to the signal from the glass substrate. For samples grown at 20 and 30 min of deposition time, figures 3(c) and (d), the measured O1s signal is clearly shifted towards lower energies and is fitted by three peaks centered close to 529.6–530.0 eV, 531.7 $\pm$ 0.1 eV and 533 $\pm$ 0.1 eV binding energies. These can be attributed to the O–Zn and OH–Zn bonds and adsorbed water, respectively. The observed shift in the measured O1s signal, for samples grown for 20 and 30 min, could be attributed to a change in the grown mechanism of the film. At the initial stages, the film formation is expected to proceed through the ion-by-ion mechanism, as suggested by the AFM analysis. However, as the reaction proceeds the $Zn(OH)_2$ is formed homogenously in the bulk of the solution and then, the film formation proceed through the cluster-by-cluster mechanism. This phenomenon is in agreement with our experimental observations during the deposition process, where the color of the reaction solution changes from translucent to white (typical for hydroxides) between 18 and 23 min.

For the signal of Zn2p$_{3/2}$ (figures 3(e)–(h)), a similar behavior is observed. Samples grown at 5 and 10 min (figures 3(e) and (f)) exhibit a peak that can be adjusted by two contributions located at around 1022.3–1022.5 eV and 1023.2 $\pm$ 0.1 eV, which are ascribed to the Zn–O bond [29, 30] and adsorbed $ZnSO_4$ [31], respectively. After 10 min of deposition time (figures 3(g) and (h)), the Zn2p$_{3/2}$ signal is shifted towards lower energies and it can be fitted by three peaks. The first one is located close to 1021.1 $\pm$ 0.1 eV and it is

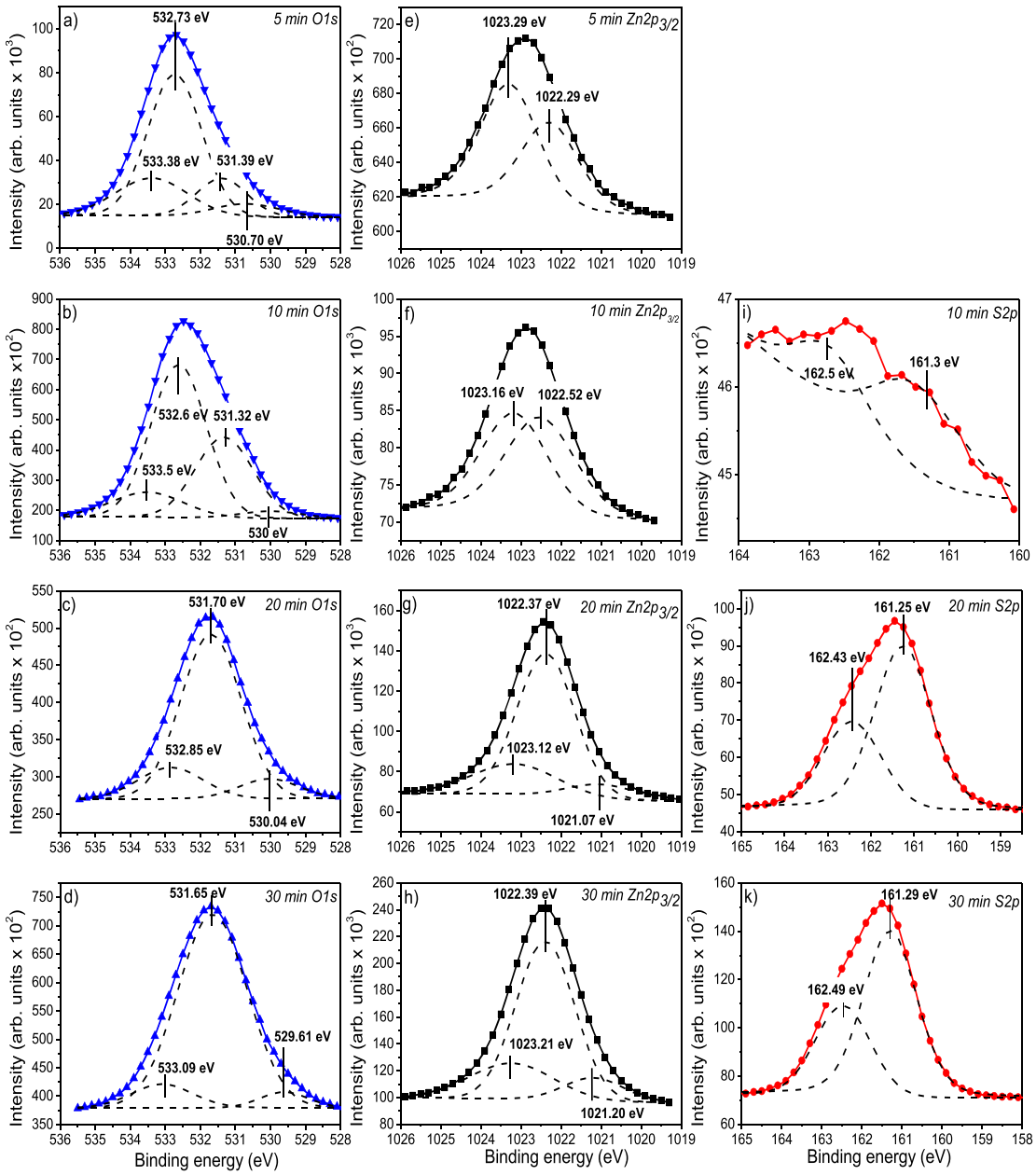

Figure 3. High–resolution XPS spectra of (a)–(d) O1s, (e)–(h) $Zn2p_{3/2}$ and (i)–(k) S2p for ZnS thin films grown at 5, 10, 20 and 30 min.

ascribed to the Zn–O bond, the second one is located at close to 1022.3 eV, which could be assigned to the Zn–OH and/or Zn–S bond. It must be noted that the identification of Zn–S bond becomes especially difficult in the presence of $Zn(OH)_2$ and ZnO. This is because the binding energies of these three compounds are very to close each other (ZnO, ZnS and $Zn(OH)_2$ are normally found at around 1021.5–1022.5 eV, 1022.0–1022.5 eV and 1021.7 $\pm$ 0.1 eV, respectively [2, 4, 12, 29, 32]). Finally, the last peak identified, is located at around 1023 eV and could be attributed to adsorbed $ZnSO_4$.

With regards to sulfur, no signal was detected in the binding energy range from 158 to 165 eV for the sample grown for 5 min. However, a clear signal was detected in the range between 164 and 172 eV (not shown here), which is attributed to the presence of the metal–SO_4 bond [21]. In addition, the absence of the Zn–S bond might be due to there being no ZnS formed or very little (lower than the XPS detection limit, 0.1 at%). It has been reported that during the early growth stages in a similar system, a very thin layer of ZnO can be deposited on the substrate surface [33–35]. The formation of this layer could explain the presence of the Zn–O bond (and the

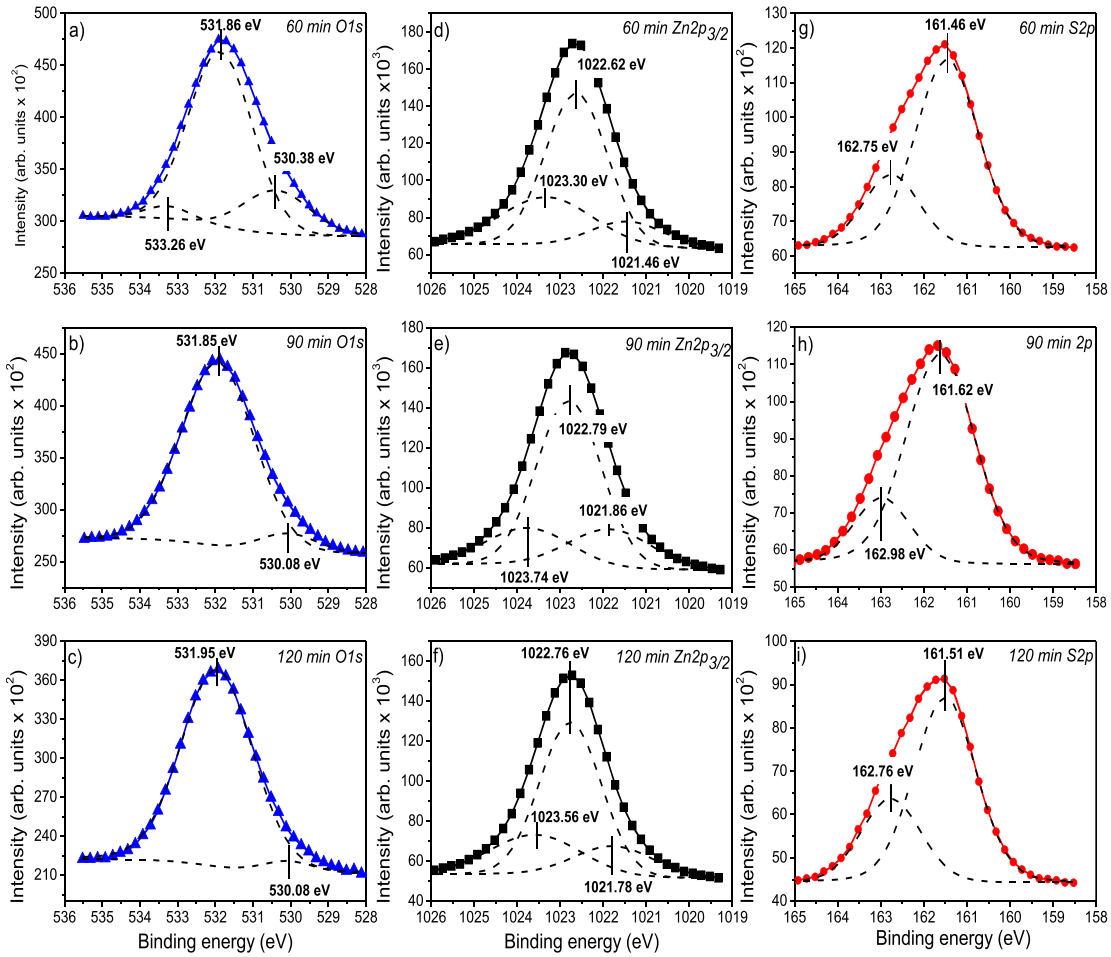

Figure 4. High–resolution XPS spectra of (a)–(c) O1s, (d)–(f) $Zn2p_{3/2}$ and (g)–(i) S2p for ZnS thin films deposited at 60, 90 and 120 min.

absence of the S–Zn bond) for the sample grown for 5 min. The growth of ZnO has been reported to proceed through the following reactions [36]:

$$Zn(CIT)_n^{2-n} + 2(OH)_{(aq)}^- \leftrightarrow ZnO + nCIT_{(aq)}^{3-} + H_2O \; n = 1, 2 \quad (6)$$

$$Zn(OH)_{n(aq)}^{(n-2)-} \leftrightarrow ZnO_{(s)} + H_2O_{(l)} + (n-2)OH_{(aq)}^- \quad (7)$$

The deposition of a ZnO film at very early growth stages during ZnS film deposition can be a consequence of both thermodynamics and kinetics. While S^{2-} ions are slowly released from thiourea, conditions are favorable for ZnO deposition (likely by equation (6)). After this, enough S^{2-} ions were released to proceed with the deposition of the ZnS film.

For films grown at higher deposition times, the presence of the S–Zn bond, due to the signal of the doublet S2p, located around 161.3 ± 0.1 eV (for 3/2) and 162.5 ± 0.1 eV (for ½) [4], is clear.

Figure 4 shows the high-resolution spectra of O1s, $Zn2p_{3/2}$ and S2p signals for ZnS thin films grown at 60, 90 and 120 min of deposition time. It can be observed that the O1s signal for the film grown at 60 min (figure 4(a)) is slightly shifted to higher energies compared with sample grown at 30 min. This could be attributed to a higher content of $Zn(OH)_2$ in the film. The signal can be fitted by three peaks located at 530.4 ± 0.1 eV, 531.9 ± 0.1 eV and 533.3 ± 0.1 eV binding energies, which can be ascribed to the O–Zn and Zn–OH bonds and water, respectively. For samples grown at 90 and 120 min (figures 4(b) and (c)), the O1s signal can be fitted by only two peaks located close to 530.1 ± 0.1 eV and 531.9 ± 0.1 eV, ascribed to the O–Zn and Zn–OH bonds, respectively. In addition, the intensity corresponding to the O–Zn bond decreases significantly. This result indicates that as the film thickness increases, the information of the very early stages of film deposition is hidden, such as the formation of the ZnO layer.

Concerning the $Zn2p_{3/2}$ signal for samples grown at 60, 90 and 120 min, figures 4(d)–(f), it is clear that no significant modifications are observed compared to samples deposited at 20 and 30 min, figures 3(g) and (h).

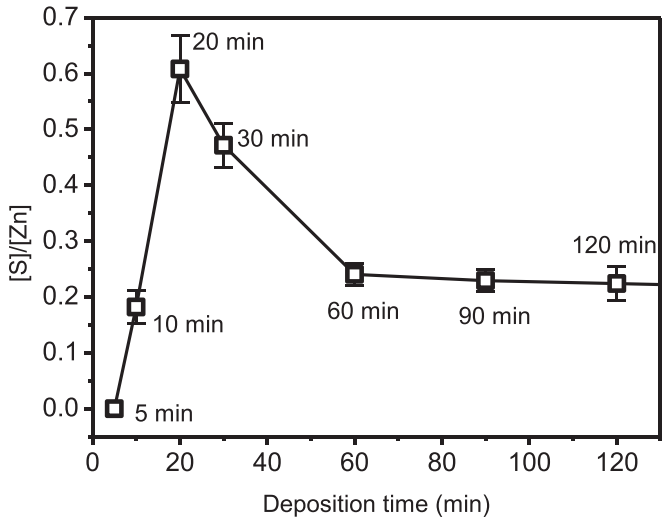

Figure 5. [S]/[Zn] ratio of the obtained ZnS thin films as a function of the deposition time.

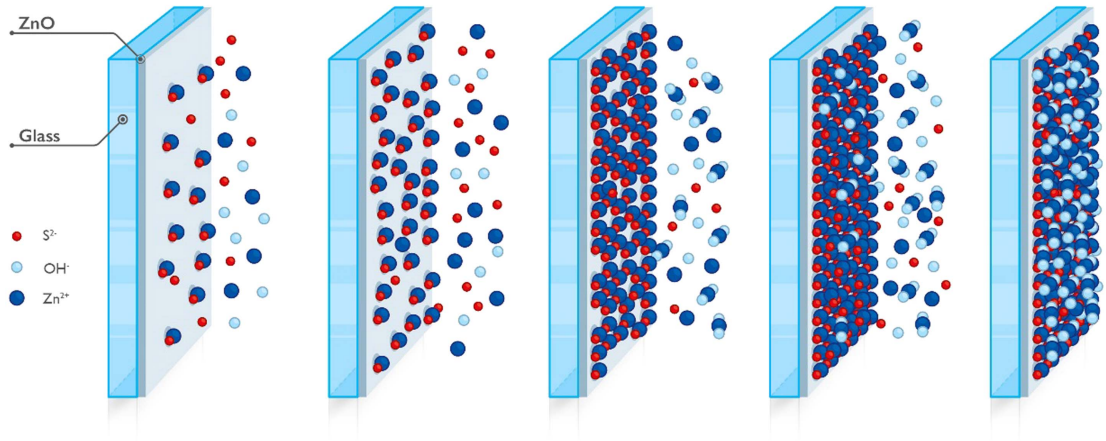

Figure 6. Scheme of the proposed growth stages for ZnS thin films.

Three peaks can be fitted corresponding to Zn–O (1021.5–1021.9 eV), Zn–OH and/or Zn–S bond (1022.7 ± 0.1 eV) and adsorbed $ZnSO_4$ (1023.3–1023.7 eV).

Figures 4(g)–(i) show the S2p signal that is associated with the formation of ZnS. No significant modification in the position of this signal was observed as the deposition time increased.

Figure 5 shows the [S]/[Zn] ratio as a function of deposition time. The relative composition was obtained using MultiPak® software [37]. The method used for quantification utilizes peak area sensitive factors and peak height sensitive factors explained in detail by Wagner *et al* [38], which consider a homogeneous sample in the analysis volume. From figure 5(a), an increment in the sulfur content can be seen as the deposition time increases. The maximum [S]/[Zn] ratio reached is 0.62 at 20 min of deposition time, after that it drastically decreases to 0.24 at 60 min of deposition time, meaning that all samples are sulfur deficient. The significant reduction on the [S]/[Zn] ratio observed between 20 and 60 min can be attributed to the constant formation and deposition of $Zn(OH)_2$. After, 60 min of deposition time, it is observed that the [S]/[Zn] ration remains almost constant.

The shape of the curve can be understood considering the change in the growth mechanism of the film, which is schematically represented in figure 6. As proposed above, at the very early growth stages, a very thin layer of ZnO is deposited on the substrate surface, resulting in a high concentration of Zn and a low concentration of S (5 and 10 min). As the reaction proceeds, ZnS starts depositing on the substrate surface mainly through the ion–by-ion mechanism. However, after 20 min, the concentration of $Zn(OH)_2$ becomes significant and then a change in the growth mechanism occurs. Although, $Zn(OH)_2$ reacts with S^{2-} ions to form ZnS (see equation (4)), the conversion to ZnS is not completed (normally attributed to steric hindrance), and

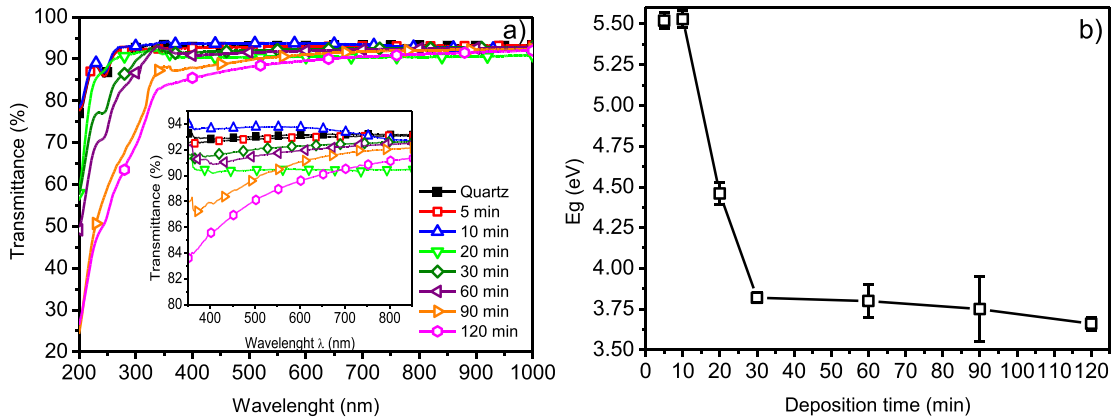

Figure 7. (a) Transmittance spectra and (b) band gap values for ZnS thin film grown at different deposition times.

$Zn(OH)_2$ is deposited likely as Zn(OH, S). This leads to a lower sulfur concentration as the deposition time increases. Finally, after 60 min of deposition time and thereafter, there is a constant [Zn]/[S] ratio, which can be attributed to a predominance of the cluster-by-cluster mechanism over the ion-by-ion mechanism. Consequently, the deposition time where the film exhibits the higher sulfur concentration was determined. Additionally, the presence of ZnO and $Zn(OH)_2$ during deposition of ZnS thin films for TFSC applications has been addressed previously, and the obtained device efficiencies were comparable to those of the corresponding Cd-containing buffer layer [39–41].

3.4. Optical properties

The optical properties of the ZnS thin films grown on quartz substrates were taken from transmittance (T) measurements in the range of 200–1000 nm. A clean quartz substrate without coating was used as a reference. Figure 7(a) shows the transmittance spectra of ZnS thin films grown at different deposition times, where the optical transmission values are higher than 85% in the visible range for all the deposited samples. It can be clearly seen that the shapes of the curves corresponding to samples grown at 5 and 10 min are almost identical to the quartz substrate, meaning that there is no ZnS thin film formation (only some nuclei and islands). Similar results have been reported in the literature [21].

Furthermore, the absorption edge is located at the UV region for all samples, and as the deposition time increases it is shifted to higher wavelengths. An absorption edge located at the UV region is desired for a buffer layer because it ensures that most of the visible radiation will be transmitted through the layer.

From the transmittance spectra, it is possible to determine the energy band gap of the films according to the methodology detailed previously [21, 42]. Figure 7(b) shows the energy band gap for the ZnS thin films grown at different deposition times, where it is observed that at 5 and 10 min, the band gap values are the same as for quartz. This agrees with the fact that during the first 10 min, there is no ZnS film formation (not a homogeneous film). At 20 min of deposition time, the band gap value of the obtained samples decreases drastically from 5.50 to 4.50 eV because of the ZnS film formation. It can be noted that this value is higher than that normally reported for ZnS thin films (below 4.2 eV), which can be attributed to the film formation process [43]. At 30 min and thereafter, the band gap values are close to 3.75 eV, and a small decrease of the value as the deposition time proceeds is observed. The shape of the curve displayed in figure 7(b) matched with the fact that as the film thickness increases, the band gap reaches, asymptotically, the band gap value of the material in bulk (3.7 eV [8]) caused by an increase in grain size [44].

Finally, it is important to note that from the above characterization, it was possible to elucidate the presence of a ZnO layer at the very early growth stages and the reason why, as the deposition time increases, this information disappears. It was also possible to determine the influence of the growth mechanism on the chemical composition, morphological and optical properties.

4. Conclusions

In this work, a morphological, chemical and optical characterization has been carried out in order to study the growth stages in ZnS thin films deposited by a non-toxic chemical bath deposition. From the morphological and chemical analysis, it is concluded that there is no homogeneous film formation before 20 min of deposition time. In addition, the formation of a ZnO layer was proposed at the very early growth stages, and that deposited

samples are always sulfur deficient. The presence of a thin layer of ZnO at the very early growth stages is a consequence of the slow release of sulfur ions from thiourea at the earliest deposition times. For the growth mechanism, it was confirmed that during the first 20 min, the film growth is carried out through the ion-by-ion mechanism. After this time, it changed to the cluster-by-cluster mechanism. The optical properties were consistent with the AFM and XPS results, and the presence of a thin layer of ZnO does not affect negatively the films properties. Finally, it is possible to optimize the deposition time of the ZnS thin films, in order to obtain a homogeneous and compact film with the higher sulfur concentration and higher band gap. The ZnS samples deposited after 20 min are excellent candidates to be used as buffer layers in thin-film solar cells.

Acknowledgments

This work was supported by CONICYT through the project FONDECYT Iniciación 11160368.

ORCID iDs

C A Rodríguez https://orcid.org/0000-0003-1237-3288

References

[1] Lekiket H and Aida M 2013 *Mater. Sci. Semicond. Proc.* **16** 1753
[2] González I and Oliva I 2016 *J. Electrochem. Soc.* **163** D421
[3] Ghezali K, Mentar K, Boudine B and Azizi A 2017 *J. Electroanal. Chem.* **794** 212
[4] Rodríguez C, Sandoval M, Cabello G, Flores M, Fernández H and Carrasco C 2014 *Mater. Res. Bull.* **60** 313
[5] Kamada R, Yagioka T, Adachi S, Handa A, Fai K, Kto T and Sugimoto H 2016 *Proc. 43rd IEEE Photovoltaic. Spec. Conf.*
[6] Abou D, Kostorz G, Romeo A, Rudmann D and Tiwari A 2005 *Thin Solid Film.* **480–481** 118
[7] Wei A, Liu J, Zhuang M and Zhao Y 2013 *Mater. Sci. Semicond. Proc.* **16** 1478
[8] Luque P, Castro A, Vilchis A, Quevedo M and Olivas A 2015 *Mater. Lett.* **140** 148
[9] Liu T, Li Y, Ke H, Qian Y, Duo S, Hong Y and Sun X 2016 *J. Mater. Sci. Tech.* **32** 207
[10] Yamaguchi K, Yoshida T, Lincot D and Minoura H 2003 *J. Phys. Chem.* B **107** 387
[11] Sandoval M and Ramírez R 2009 *Thin Solid Film.* **517** 6747
[12] Hong J, Lim D, Joo Y and Choi C 2017 *Appl. Surf. Sci.* **432** 250
[13] Horcas I, Fernandez R, Gomez J, Colchero J, Gomez J and Baro A 2007 *Rev. Sci. Instrum.* **78** 13705
[14] Hodes G 2002 *Chemical Solution Deposition of Semiconductor Films* (New York: Marcel Dekker)
[15] Ishizaki T, Ohomoto T, Sakamoto Y and Fuwa A 2004 *Mater. Trans.* **45** 277
[16] Krotz R, Evangelou B and Wagner G 1989 *Plant. Physiol.* **91** 780
[17] Antony A, Murali K, Manoj R and Jayaraj M 2005 *Mater. Chem. Phys.* **90** 106
[18] Cheng Q, Wang D and Zhou H 2017 *J. Energy Chem.* **27** (2018) 913
[19] Rodríguez C, Tobosque P, Maril M, Camurri C, Basáez L and Delplancke M 2017 *J. Mater. Sci.* **52** 3388
[20] Tobosque P, Maril M, Maril Y, Camurri C, Delplancke J, Delplancke M, Rodríguez C and Carrasco C 2017 *J. Electrochem. Soc.* **164** D621
[21] Mazón D, Sotelo M, Quevedo M, El-Bouanani M, Alshareef H, Esponiza F and Ramirez R 2007 *Appl. Surf. Sci.* **254** 499
[22] Das N, Roy D, Clarke N, Ganesan V and Gupta P 2014 *RSC Adv.* **4** 32490
[23] Hosseinpanahi F, Raoufi D, Ranjbarghanei K, Karmi B, Babaei R and Hasani E 2015 *Appl. Surf. Sci.* **357** 1843
[24] Sandoval M, Sotelo M, Mendoza A and Ramírez R 2007 *Thin Solid Film.* **515** 3356
[25] Eisele W, Ennaoui A, Schubert P, Giersig M, Pettenkofer C, Karuser J, Lux M, Zweigar S and Karg F 2003 *Solar Energy Mater. Solar Cells* **75** 17
[26] He H, Alberti K, Barr T and Klinowski J 1993 *J. Phys. Chem.* **97** 13703
[27] Chao S, Takagi Y, Lukovsky G, Pai P, Caster R, Tyler J and Keem J 1986 *Appl. Surf. Sci.* **26** 575
[28] Yu F, Ou S, Yao P, Wu B and Wuu D 2014 *J. Nanomater.* **2014** 594952
[29] Wehner P, Mercer P and Apai G 1983 *J. Catal.* **84** 244
[30] Gaarenstroom S and Winograd N 1977 *J. Chem. Phys.* **67** 3500
[31] Nefedov V 1982 *J. Electron Spectrosc. Relat. Phenom.* **25** 29
[32] Deroubaix G and Marcus P 1992 *Surf. Interface Anal.* **18** 39
[33] Kokotov M and Hodes G 2010 *Chem. Mater.* **22** 5483
[34] Buffière M, Gautron E, Hildebrandt T, Harel S, Guillot-Deudon C, Arzel L, Naghavi N and Kesseler J 2013 *Thin Solid Film.* **535** 171
[35] Hubert C, Naghavi N, Canava B, Etcheverry A and Lincot D 2007 *Thin Solid Film.* **515** 6032
[36] Rosado M, Oliva A and Oliva A 2018 *Thin Solid Film.* **645** 231
[37] López M, Espios J, Martín F, Leinen D and Ramos J 2005 *J. Cryst. Grown* **285** 66
[38] Wagner C, Ringgs W, Davis L and Moulder J 1979 ed G E Muilenberg *Handbook of X-Ray Photoelectron Spectroscopy* (Minesota: PerkinElmer Corporation)
[39] Contreras M, Nakada T, Hongo M, Pudov A and Sites J 2003 *3er World Conf. Photovoltaic Energy Convers (May 11–18) (Osaka, Japan p 570*
[40] Ichiboshi A, Hongo M, Akamine T, Dobashi T and Nakada T 2006 *Solar Energy Materials and Solar Cells* **90** 3130
[41] Hultquivst A, Platzer C, Coronel E and Edoff M 2011 *Solar Energy Mater. Solar Cells* **95** 497
[42] Ochoa R, Sandoval M, Ortuño M, Sotelo M and Ramírez R 2009 *J. Phys. Chem. Solid.* **70** 1034
[43] Mazón D, Sotelo M, Rodríguez L and Huerta L 2010 *Appl. Surf. Sci.* **256** 4280
[44] Moubah R, Colis S, Gallart M, Schmerber G, Gilliot P and Dinia A 2012 *J. Lumin* **132** 458